Journal of Ginseng Research 47 (2023) 81–88

Contents lists available at ScienceDirect

Journal of Ginseng Research

journal homepage: https://www.sciencedirect.com/journal/journal-of-ginseng-research

Research Article

Respiratory protective effects of Korean Red Ginseng in a mouse model of particulate matter 4-induced airway inflammation

Won-Kyung Yang [a, b], Sung-Won Kim [c], Soo Hyun Youn [c], Sun Hee Hyun [c], Chang-Kyun Han [c], Yang-Chun Park [a], Young-Cheol Lee [d], Seung-Hyung Kim [b, *]

[a] Division of Respiratory Medicine, Department of Internal Medicine, College of Korean Medicine, Daejeon University, Daejeon, Republic of Korea
[b] Institute of Traditional Medicine and Bioscience, Daejeon University, Daejeon, Republic of Korea
[c] Laboratory of Efficacy Research, Korea Ginseng Corporation, Daejeon, Republic of Korea
[d] Department of Herbology, College of Korean Medicine, Sangji University, Wonju, Republic of Korea

ARTICLE INFO

Article history:
Received 27 July 2021
Received in revised form
25 January 2022
Accepted 23 May 2022
Available online 14 June 2022

Keywords:
Airway inflammation
Korean Red Ginseng
Korean Red Ginseng extract
Particulate matter
PM4+D-induced respiratory disease model
21

ABSTRACT

Background: Air pollution has led to an increased exposure of all living organisms to fine dust. Therefore, research efforts are being made to devise preventive and therapeutic remedies against fine dust-induced chronic diseases.

Methods: Research of the respiratory protective effects of KRG extract in a particulate matter (PM; aerodynamic diameter of <4 μm) plus diesel exhaust particle (DEP) (PM4+D)-induced airway inflammation model. Nitric oxide production, expression of pro-inflammatory mediators and cytokines, and IRAK-1, TAK-1, and MAPK pathways were examined in PM4-stimulated MH-S cells. BALB/c mice exposed to PM4+D mixture by intranasal tracheal injection three times a day for 12 days at 3 day intervals and KRGE were administered orally for 12 days. Histological of lung and trachea, and immune cell subtype analyses were performed. Expression of pro-inflammatory mediators and cytokines in bronchoalveolar lavage fluid (BALF) and lung were measured. Immunohistofluorescence staining for IRAK-1 localization in lung were also evaluated.

Results: KRGE inhibited the production of nitric oxide, the expression of pro-inflammatory mediators and cytokines, and expression and phosphorylation of all downstream factors of NF-κB, including IRAK-1 and MAPK/AP1 pathway in PM4-stimulated MH-S cells. KRGE suppressed inflammatory cell infiltration and number of immune cells, histopathologic damage, and inflammatory symptoms in the BALF and lungs induced by PM4+D; these included increased alveolar wall thickness, accumulation of collagen fibers, and TNF-α, MIP2, CXCL-1, IL-1α, and IL-17 cytokine release. Moreover, PM4 participates induce alveolar macrophage death and interleukin-1α release by associating with IRAK-1 localization was also potently inhibited by KRGE in the lungs of PM4+D-induced airway inflammation model. KRGE suppresses airway inflammatory responses, including granulocyte infiltration into the airway, by regulating the expression of chemokines and inflammatory cytokines via inhibition of IRAK-1 and MAPK pathway.

Conclusion: Our results indicate the potential of KRGE to serve as an effective therapeutic agent against airway inflammation and respiratory diseases.

1. Introduction

Industrial development and rapid economic growth have improved the quality of life of humans, and medical technologies have prolonged life expectancy. However, the rapid industrial development has led to an increase in environmental air pollution, which have a significant public health impact [1,2]. Among the diverse air pollutants, particulate matter (PM) is a global environmental issue and has been recently recognized as one of the most serious health threats owing to its small size and toxicity [3,4]. Based on its aerodynamic diameter, PM is crudely categorized as coarse PM that has an aerodynamic diameter of 2.5–10 μm, fine PM that has an aerodynamic diameter of <2.5 μm, and ultrafine PM that has an aerodynamic diameter of <0.1 μm. Each type of PM has a

* Corresponding author. Institute of Traditional Medicine and Bioscience, Daejeon University, Daejeon, 34520, Republic of Korea.
E-mail address: sksh518@dju.kr (S.-H. Kim).

https://doi.org/10.1016/j.jgr.2022.05.008

distinct composition and exerts different effects on human health including respiratory symptoms [5,6]. When PM is inhaled, it is deposited on the surface of the lungs and attached to the pulmonary epithelial cells, leading to the induction of various respiratory disease [7,8]. PM exposure has been reported to exacerbate asthma and chronic obstructive pulmonary disease, increase the incidence of lung cancer, alter lung function, and cause diverse respiratory disease [9]. In addition, PM is known to cause abnormal inflammatory and coagulation responses in the entire body [10,11]. For this reason, despite the growing global interest in PM and the increasing number of related studies, effective therapeutic agents against PM are yet to be identified [12]. Therefore, there is an urgent need for novel preventive and therapeutic agents that can protect against PM-induced respiratory damage.

The traditional Korean medicine, Korean Red Ginseng, is used to improve health. There are different biological effects from the major components of ginseng, saponin and 37 ginsenosides. Some of the effects are anti-inflammatory, anti-allergic, and antitumor activities [13–17]. KRG showed anti-allergic effects in allergic mouse models and reduced Th2 cytokine activity [18]. Ginsenoside Rd evokes Th1 and Th2 immune responses via regulating the expression of Th1 and Th2 cytokines [19]. Ginsenosides Rh1, Rh2, Rg1, Rg3 exert anti-inflammatory effects that are regulated by various cytokines, histamine, IgE, and IgG1 levels, and eosinophil and mast cell infiltration. In addition, they have been found to be effective in an animal model of atopic dermatitis and allergic rhinitis [20–24]. However, no data has been found on the effects of KRG on inflammation induced by PM4, DEP, and combustion particles. In the present study, we focused on KRG, which has been used for centuries in Oriental countries. We investigated the respiratory protective effects of KRGE in a PM4+D-induced murine airway inflammation model.

2. Materials and methods

2.1. Cell viability assay and nitric oxide

For the cell viability assay, MH-S cells were incubated in 96-well plates in the presence or absence of 20 μg/mL PM4 for 16 h; then, the extract was added. 24 h later, MTT assay was performed. MH-S cells were incubated for 16 h to evaluate the inhibitory activity of KRGE on PM4-induced NO production; then, the extract was added, followed by 20 μg/mL PM4. NO production was measured indirectly using Griess reagent to assess the accumulation of nitrite [25].

2.2. Western blot analysis

MH-S cells were treated or not treated with KRGE in the presence or absence of 40 μg/mL PM4. The membranes were then incubated with specific primary antibodies against phospho- and/or total ERK, JNK, p38, TAK, IRAK1. Which was then followed by a 1 h incubation with horseradish peroxidase-conjugated anti-rabbit antibody. The bound antibodies were observed using enhanced chemiluminescence, and images were analyzed using Image J software. The internal control used was β-actin.

2.3. Animals and treatments

Male BALB/c mice were procured from The Jackson Laboratory (Bar Harbor, ME, USA). The committee for animal welfare at Daejeon University (DJUARB2019 019) approved the study protocol and was performed in exacting accordance with committee guidelines.

Mice were orally treated with KRGE every other day for 12 d and intranasal administration with fine dust (PM4, SRM 24786, National Institute of Standards and Technology Company, Gaithersburg, MD, USA; DEP, SRM 2975, National Institute of Standards and Technology Company, Gaithersburg, MD, USA) complex solution (PM4 and DEP: PM4+D) on days 4, 7, and 10. PM4 (7.5 mg/mL) and DEP (0.6 mg/mL) were dissolved in 1% aluminum hydroxide gel adjuvant. On day 12, blood, BALF, and lung tissues were collected from euthanized mice for further experiments. Fig. 2A is a schematic diagram of the experimental set-up.

2.4. Blood cell counts

Blood was collected to analyze white blood cell count and WBC differential count using a CELL-DYN® 3200 analyzer (Abbott Laboratories, Santa Clara, CA, USA).

2.5. Collection of BALF and cytospin cell count

To isolate BALF from the trachea and lungs, a syringe was inserted into the trachea and airways of anesthetized mice and the fluid was aspirated. A cytospin centrifuge was used to spin onto glass slides. A Diff-Quick Stain Kit was used to determine differential cell counts.

2.6. Measurement of inflammatory mediators in BALF

The levels of MIP2, TNF-α, IL-17A, IL-1α, and CXCL-1 in BALF were determined using ELISA kits according to the manufacturer's protocol.

2.7. Digestion of pulmonary tissue and cell preparations

After the lungs were extracted from the thoracic cavity, the tissues were minced using a sterile scalpel. The tissues were then incubated in collagenase IV and dispase at 37 °C on a shaker. After a 30–40 min incubation, the lung tissues were actively pipetted up and down to further dissolve the remaining tissue clumps and filtered using a 70 μm pore size nylon cell strainer and centrifuged for 20 min at 450 x G. Total cell numbers were determined using a hemocytometer.

2.8. Flow-cytometric analysis

Cells from the lungs and BALF were incubated with fluorescein isothiocyanate and phycoerythrin-labeled monoclonal antibodies for Anti-CD3, anti-CD4, anti-CD8, anti-CD69, anti-CD11b, and anti-granulocytic marker GR1 for 30 min. Afterwards, they were washed with PBS, fixed with 0.5% paraformaldehyde for 20 min, washed again with PBS, and analyzed in two-color flow cytometry on a FACS Calibur using the CellQuest software (BD Biosciences, San Diego, CA). Quantitative reverse-transcription RT-qPCR.

Total RNA from MH-S cells with KRGE for 30 min followed by stimulation with 20 μg/mL PM4 for 18 h and lung tissues of mice with PM4-induced airway were isolated with TRIzol® and digested with DNase I to remove chromosomal DNA. The qPCRs were run in duplicate using the SYBR Green PCR Master Mix 200 nM primers an Applied Biosystems 7500 Real-Time PCR system according to the manufacturer's instructions.

2.9. Immunohistofluorescence staining

Lung tissues were frozen at −20 °C, and sections of 20 μm thickness were cut using a Cryostat Microtome (CM 3050S; Leica Microsystems, Wetzlar, Germany). Double immunofluorescence staining was performed by incubating the sections with an antibody targeting IRAK-1, CD11b, MCP-1, TNF-α at 4 °C overnight. The sections were observed under an Eclipse Ti-E inverted fluorescence

microscope (Nikon Instruments Inc., Mississauga, Canada). Image J software was used in three independent experiments to obtain the mean fluorescence intensity quantified from images.

2.10. Histopathological analysis of lung and tracheal tissues

Lung tissue sections were stained with hematoxylin–eosin and Masson's trichrome staining. In order to find the severity of inflammatory cell infiltration, peribronchial cell count, mucus production, and goblet cell hyperplasia were quantified in the airway epithelium in a blind manner using a 5-point (0–4) grading system [32,33].

2.11. Statistical analysis

Analysis of data was achieved using unpaired Student's *t*-test or one-way analysis of variance followed by Dunnett's multiple comparison test using SPSS version 14.0. Results are presented as the mean ± SEM, and significant differences are denoted as $^{\#}p < 0.05$, $^{\#\#}p < 0.01$, and $^{\#\#\#}p < 0.001$ (compared to non-treated control) and $*p < 0.05$, $**p < 0.01$, and $***p < 0.001$ (compared to PM4+D_CTL).

3. Results

3.1. Cytotoxic activity and effect of KRGE on NO production in MH-S cells

The cytotoxicity of KRGE against MH-S cells was assessed using the MTT assay. After a 24 h incubation, no cytotoxicity was observed in the KRGE-treated groups (Fig. 1A). Fig. 1B and C shows that KRGE hindered the production of nitrite and expression of pro-inflammatory mediators and cytokines such as iNOS in a dose-dependent manner. This inhibition of NO production did not appear to be due to cytotoxicity, because the MTT assay indicated that KRGE does not kill MH-S cells at the concentrations used. As shown in Fig. 1D and E, IRAK-1 protein expression and phosphorylation of MAPKs/AP-1 were inhibited by KRGE.

3.2. Effect of KRGE on neutrophil count in BALF and tissue damage in lung tissues

The total numbers of cells in BALF were considerably decreased, but the total number of cells in lung did not by KRGE and Dexa treatment (Fig. 2B and C). Also, KRGE and Dexa treatment showed significantly lower neutrophil/eosinophil infiltration than control group (Fig. 2D and E). On the other hands, during the airway inflammation, neutrophils, eosinophils, and activated macrophages intensified inflammation, leading to the destruction of alveolar cells, collagen deposition, and goblet cells that secrete mucus around the airway. Histological sections of lung and tracheal tissues revealed that Dexa and KRGE reduced the degree of inflammation around the bronchus and the mucus content in respiratory epithelial cells, which was suppressed to levels close to that in the non-treated control group (Fig. 2F–H, Fig. 2G–I).

3.3. Effect of KRGE on blood leukocytes

KRGE treatment increased the number of white blood cells and lymphocytes. Also, the number of neutrophils, eosinophils, and monocytes decreased by KRGE treatment (Fig. 3A–C).

3.4. Effect of KRGE on number of immune cells in lung and BALF tissues

KRGE intensively suppressed the number of total immune cells and neutrophils in the lung and BALF samples. To evaluate the effect of KRGE on immune cell subtypes, a flow-cytometric analysis was performed and found the absolute numbers of $CD3^{-}$, $CD4^{-}$, $CD19^{-}$, CD62L-, CD107a-, $CD69^{-}$, CD11b-, and Gr-1-positive cells in

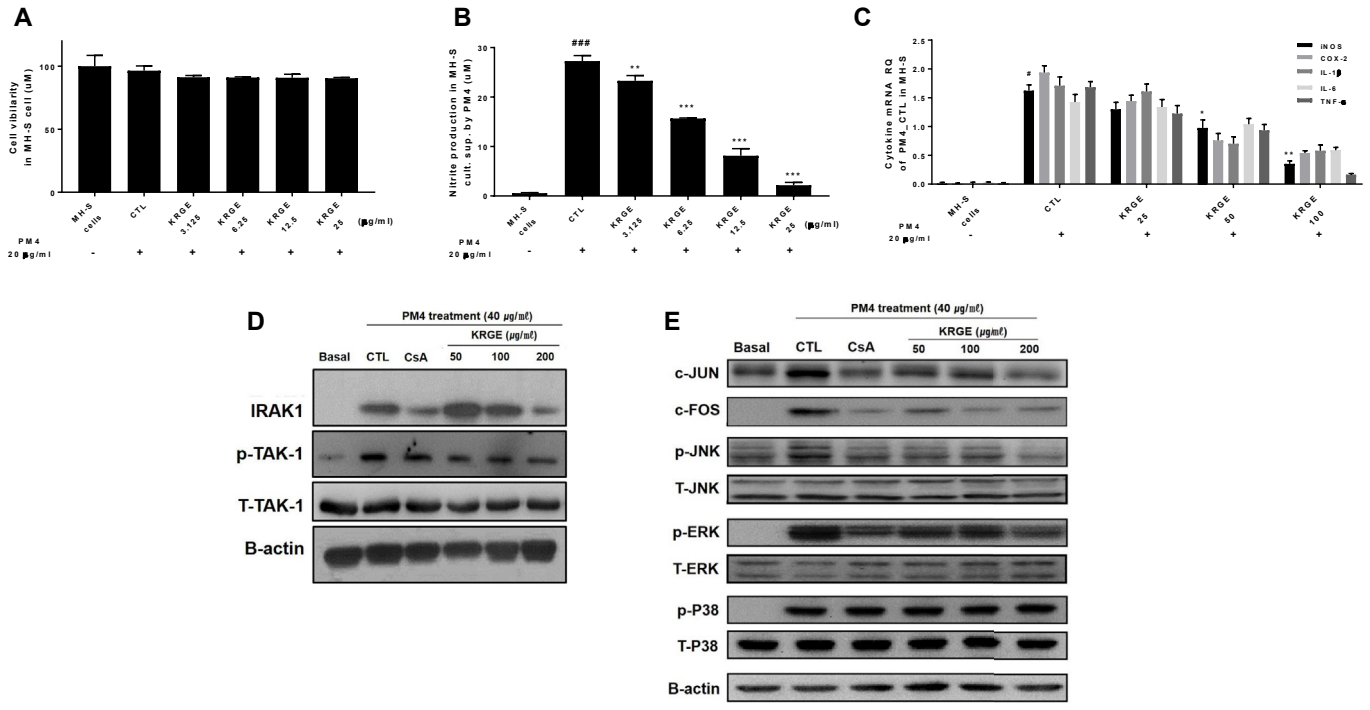

Fig. 1. Effects of KRGE on signal transduction via the NF-κB and MAPK pathways in MH-S cells *in vitro*. (A) Cell viability, (B) Nitrite production, and (C and D) IRAK and MAPK Signal pathway. Data are expressed as mean ± SEM. PM4: particulate matter (diameter <4 μm); KRGE: Korean Red Ginseng extract; CsA: cyclosporine A.

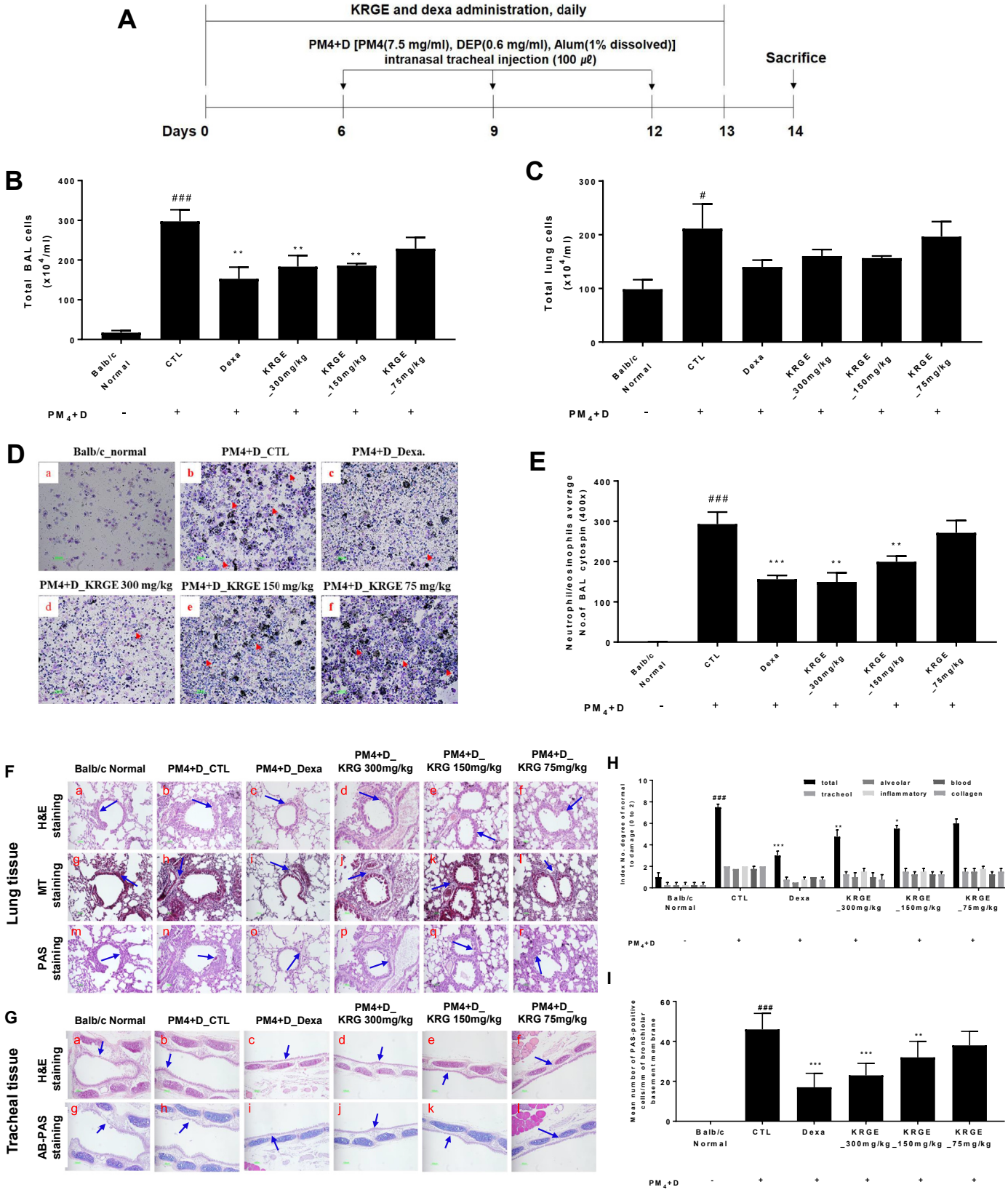

Fig. 2. Effects of KRGE and Dexa on airway immune cell number and neutrophilic airway inflammation in a PM4+D-induced airway inflammation murine model. (A) Scheme of the PM4+D sensitization and challenge protocol. Mice were exposed to 100 μ L of PM4+D mixed solution by intranasal tracheal injection, thrice, with 3-d intervals, for 12 d. (B) Total BALF cells in each treatment group. (C) Total lung cells in each treatment group. (D) KRGE suppressed neutrophils in BALF. (E) Photomicrograph of BALF cytospins from mice with PM4+D-induced airway inflammation (magnification, 200 ×), (F)(H) Histological analysis (H&E, MT, and PAS staining) of lung tissues of PM4+D-induced airway inflammation model mice. (G)(I)Histological analysis (H&E, AB-PAS staining) of tracheal tissue of PM4+D-induced airway inflammation model mice (a) BALB/c normal, (b) PM4+D-sensitized control mice, (c) 3 mg/kg dexamethasone-treated PM4+D-sensitized mice, (d) 300 mg/kg KRGE-treated PM4+D-sensitized mice, (e) 150 mg/kg KRGE-treated PM4+D-sensitized mice, and (f) 75 mg/kg KRGE-treated PM4+D-sensitized mice. Data are from individual mice, with arithmetic mean points shown in histograms. Data are expressed as the mean ± SEM.

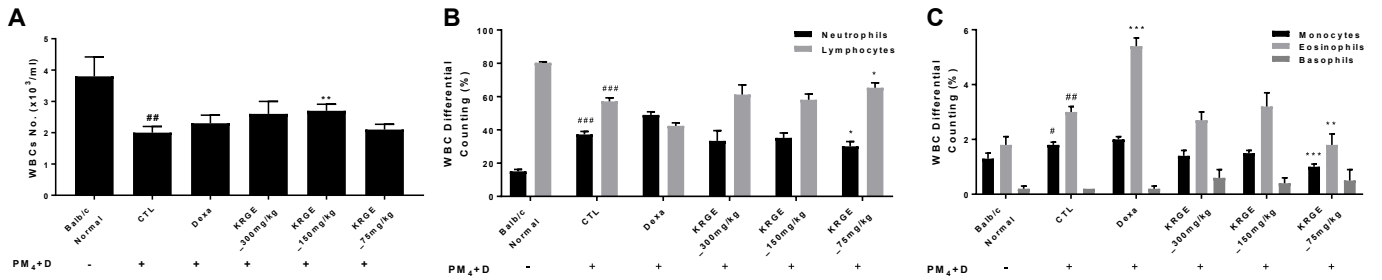

Fig. 3. Effects of KRGE on WBC and WBC differential counts in blood of a PM4+D-induced airway inflammation murine model. (A) WBC number, (B) percentage of neutrophils and lymphocytes, (C) percentage of monocytes, eosinophils, and basophils in neutrophils and lymphocytes in the blood. Data are expressed as the mean ± SEM.

Table 1
Sequence of probes for Real-Time PCR.

Gene	Primer	Oligonucleotide sequence
GAPDH	F	5′-CAATGAATACGGCTACAGCAAC-3′
	R	5′-AGGGAGATGCTCAGTGTTGG-3′
iNOS	F	5′-CCCTTCCGAAGTTTCTGGCAGCAGC-3′
	R	5′-GGCTGTCAGAGCCTCGTGGCTTTGG-3′
CXCL-1	F	5′-ATCCAGAGCTTGAAGGTGTTG-3′
	R	5′-GTCTGTCTTCTTTCTCCGTTACTT-3′
COX-2	F	5′-TCTCAGCACCCACCCGCTCA-3′
	R	5′-GCCCCGTAGACCCTGCTCGA-3′
MIP2	F	5′-GGGAGAGGGTGAGTTGGG-3′
	R	5′-GCACACTACTTCCATGAAAGC-3′
TNF-α	F	5′-TTGACCTCAGCGCTGAGTTG-3′
	R	5′-CCTGTAGCCCACGTCGTAGC-3′
IL-6	F	5′-GTACTCCAGAAGACCAGAGG-3′
	R	5′-TGCTGGTGACAACCACGGCC-3′
IL-17	F	5′-TCTCATCCAGCAAGAGATCC-3′
	R	5′-AGTTTGGGACCCCTTTACAC-3′
TRPA1	F	5′-ATTGTTCTCATGAACTTACTGATTGGCT-3′
	R	5′-CCTGGGTCTATTTGGATACACGAT-3′
TRPV1	F	5′-TTGGATTTTCCACAGCCGTAGT-3′
	R	5′-GAACTTGAACAGCTCCAGACATGT-3′
MUC5AC	F	5′-AGAATATCTTTCAGGACCCCTGCT-3′
	R	5′-ACACCAGTGCTGAGCATACTTTT-3′

3.5. Effects of KRGE on pro-inflammatory cytokine expression in the BALFand lung

Pro-inflammatory cytokines are secreted in response to inflammation, and their timely control is critical. If the secretion of these chemicals is uncontrolled, tissues will be irreparably damaged. Fig. 4A–E illustrates that KRGE and Dexa treatment significantly suppressed the levels of IL-17, TNF-α, MIP2, IL-1α, and CXCL-1 in BALF of PM4+D-induced mice. In addition, CXCL-1, MUC5AC, TRPA1, TRPV1, TNF-α, IL-17, COX-2, IL-6, MIP2, and NOS II transcript levels were reduced by KRGE and Dexa treatment in the lung tissues of PM4+D-induced mice (Fig. 4F-O). These results demonstrated that KRGE affects cytokine levels in PM4+D-induced mice.

3.6. Inhibition of fluorescence intensity of IRAK-1, MCP-1, and TNF-α

IRAK-1 and CD11b that play an important role in regulating the inflammatory pathway. MCP-1 is an important regulator of the gene expression of pro-inflammatory mediators, such as IRAK-1 and TNF-α. IRAK-1- and CD11b-positive cells (Fig. 5A–C), and

Table 2
Effects of KRGE on airway immune cell number and neutrophilic airway inflammation in PM4+D-induced airway inflammation murine model.

Cell phenotypes in Lung, BALF		PM4-induced airway inflammation murine model (Absolute No.)					
		Normal BALB/c (WT)	PM4+D_CTL	PM4+D_Dexa	PM4+D_KRG 300 mg/kg	PM4+D_KRG 150 mg/kg	PM4+D_KRG 75 mg/kg
Neutrophils (× 10^5 cells)	Lung	25.74 ± 3.03	103.24 ± 24.33$^{\#\#}$	71.39 ± 10.36	74.0 ± 1.1	80.11 ± 4.3	73.66 ± 16.64
Gr-1$^+$/CD11b$^+$ (× 10^5 cells)		7.18 ± 0.68	34.56 ± 11.88$^{\#}$	19.02 ± 2.91	19.89 ± 0.79	19.27 ± 0.29	25.10 ± 7.12
CD3e$^+$/CD19$^-$ (× 10^5 cells)		61.45 ± 12.21	128.53 ± 28.40$^{\#}$	81.83 ± 6.27	99.22 ± 7.99	96.3 ± 3.43	118.78 ± 11.84
CD4$^+$/CD69$^+$ (× 10^5 cells)		11.15 ± 1.4	29.52 ± 4.06$^{\#\#\#}$	16.47 ± 2.27**	18.48 ± 2.27*	19.26 ± 2.61*	28.72 ± 4.23
CD3$^+$/CD4$^+$ (× 10^5 cells)		39.13 ± 6.99	85.73 ± 18.12$^{\#}$	48.39 ± 4.83	62.36 ± 8.94	59.75 ± 4.86	81.13 ± 9.56
CD4$^+$/CD62L$^+$/CD107a$^+$ (× 10^5 cells)		2.57 ± 0.64	3.75 ± 0.87	4.08 ± 0.64	10.21 ± 0.21***	7.66 ± 0.49**	8.44 ± 2.05*
Neutrophils (× 10^4 cells)	BALF	5.27 ± 1.71	269.52 ± 25.37$^{\#\#\#}$	132.61 ± 23.53**	149.0 ± 26.94**	156.15 ± 2.81***	194.46 ± 22.43*
CD3$^+$/CD4$^+$ (× 10^4 cells)		1.14 ± 0.33	104.81 ± 11.81$^{\#\#\#}$	31.94 ± 1.14***	52.87 ± 10.33**	56.32 ± 3.18**	72.62 ± 10.07*
CD4$^+$/CD69$^+$ (× 10^4 cells)		2.33 ± 1.7	69.57 ± 5.4$^{\#\#\#}$	21.44 ± 0.81***	32.86 ± 2.37***	38.77 ± 2.74***	51.84 ± 8.47
Gr-1$^+$/CD11b$^+$ (× 10^4 cells)		1.86 ± 0.43	241.97 ± 21.7$^{\#\#\#}$	115.86 ± 19.05***	123.76 ± 23.83**	128.55 ± 7.83***	185.86 ± 19.88

Fluorescence-activated cell sorting analysis (FACS) of immune cell subtypes in the lungs and BALF was undertaken.
Data are expressed as the mean ± SEM (n = 6). $^{\#}p < 0.05$, $^{\#\#}p < 0.01$, and $^{\#\#\#}p < 0.001$ (compared to Balb/c Normal), and $^{*}p < 0.05$, $^{**}p < 0.01$, and $^{***}p < 0.001$ (compared to PM4+D). BALB/c normal, PM4+D-sensitized control mice, 3 mg/kg dexamethasone-treated PM4+D-sensitized mice, 300 mg/kg KRGE-treated PM4+D-sensitized mice, 150 mg/kg KRGE-treated PM4+D-sensitized mice, and 75 mg/kg KRGE-treated PM4+D-sensitized mice.

the lungs and BALF of KRGE treatment. This finding indicated that the hyperactivation of the immune system caused by PM4+D was effectively suppressed by KRGE, thereby reducing the aggravation of inflammation (Table 1) (see Table 2).

MCP-1 and TNF-α-positive cells (Fig. 5D–G) were potently inhibited in lung tissues of mice treated with Dexa and KRGE treatment strongly inhibited this response. These results suggested that KRGE exerts anti-inflammatory effects on PM4+D-induced airway inflammation.

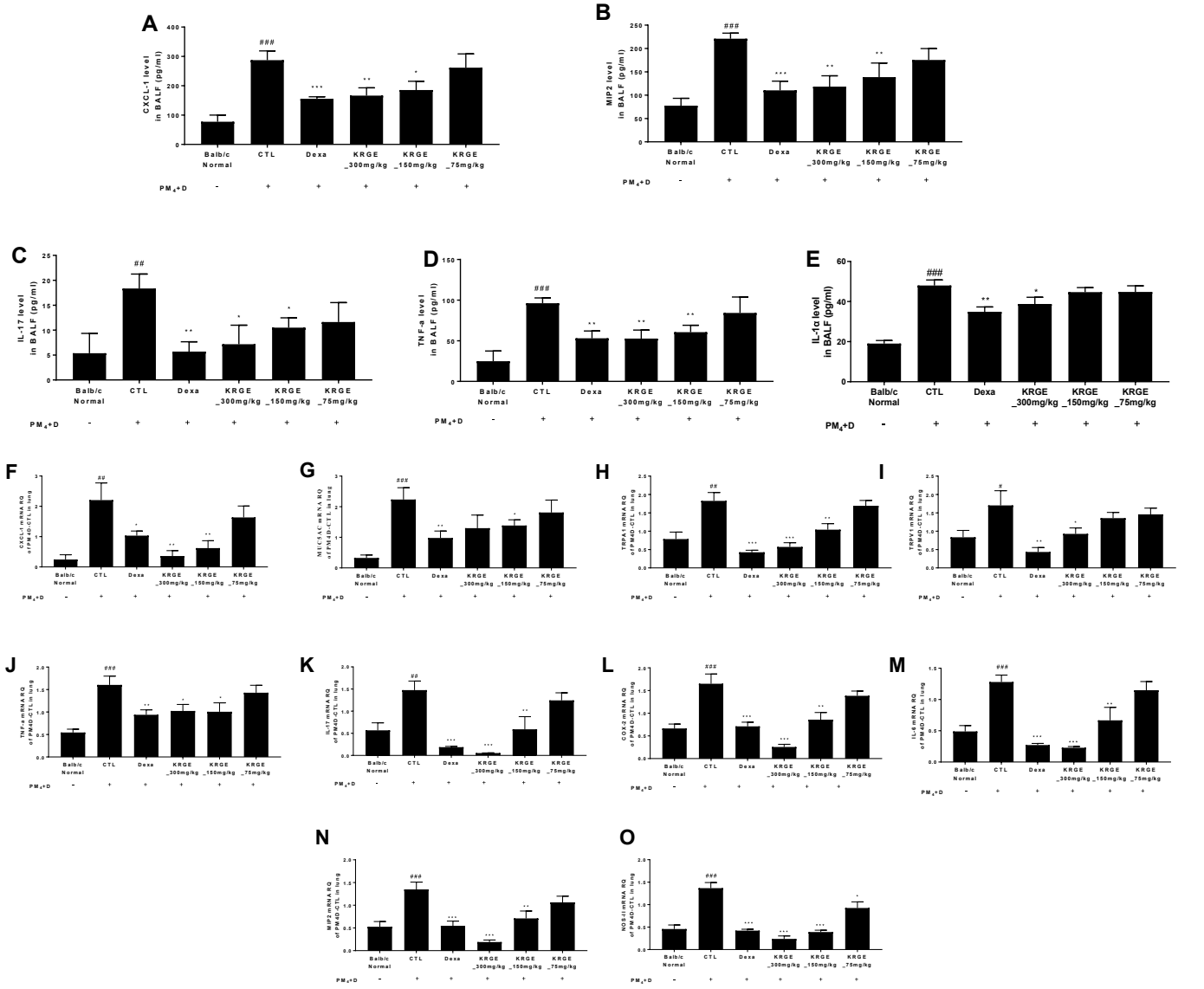

Fig. 4. Effects of KRGE on pro-inflammatory cytokines in BALF and lung tissues. KRGE reduced (A) CXCL1, (B) MIP2, (C) IL-17A, (D) TNF-α and (E) IL-1α levels in the BALF collected from WT-, PM4+D-, dexamethasone (3 mg/kg)-, and KRGE (300 mg/kg, 150 mg/kg, 75 mg/kg)-treated mice as measured using ELISA. Data are from individual mice, with arithmetic mean points shown in histograms. Effects of KRGE on cytokine mRNA expression in lung tissues. (F) CXCL-1, (G) MUC5AC, (H) TRPA1, (I) TRPV1, (J) TNF-α, (K) IL-17, (L) COX-2, (M) IL-6, (N) MIP2, and (O) NOS expression was determined using RT-qPCR. Expression is presented as relative quantitation (RQ). Data are from individual mice, with arithmetic mean points shown in histograms. Values are expressed as mean ± S.E.M.

4. Discussion

Due to the air pollution caused by industrial and urban developments, all living organisms are inevitably increasingly exposed to fine dust particles. Therefore, researchers have been attempting to identify preventive and therapeutic strategies against fine dust-induced chronic diseases. In the study, we aspired to determine the respiratory protective effects of KRGE in a PM4+D-induced airway inflammation mouse model, and found KRGE to be a potential therapeutic agent against respiratory diseases caused by inhalation of PM4+D. PM4+D exposure induces various histopathological changes, including elevated epithelial thickness and evident recruitment of leukocytes, goblet cell hyperplasia, erosion in perivascular and peribronchial areas, damaged alveolar wall, and pulmonary bullae [26]. We observed that KRGE reduced airway inflammation, alveolar dilatation and airway wall thickening. Moreover, KRGE alleviated the pathological injury of trachea induced by PM4+D. These results indicate that KRGE can protect the damage of lung and trachea against PM4+D-induced histopathological changes. An increase in the number of immune cells in BALF and lung cells and in the expression of pro-inflammatory cytokines in the lungs were induced by PM [27]. Inhalation of DEP exacerbates allergen-related eosinophil recruitment and airway hyperresponsiveness in mice [28]. We observed a significant decrease in the neutrophil, monocyte and eosinophil number in blood, numbers of neutrophil, various immune cells including $CD3^-$, $CD4^-$, $CD19^-$, CD62L-, CD107a-, $CD69^-$, CD11b-, and Gr-1-positive cells in the lungs and BALF monocyte of BAL and lung cells. Neutrophils play a key role in the PM-mediated recruitment of inflammatory cells to the airway and are considered a hallmark of pulmonary inflammation [29–31]. CD4 is involved in cell-mediated immunity, macrophage activation, maturation of B cells, and allergic inflammation. CD8 plays an important role in immunity, including cell-mediated immunity and

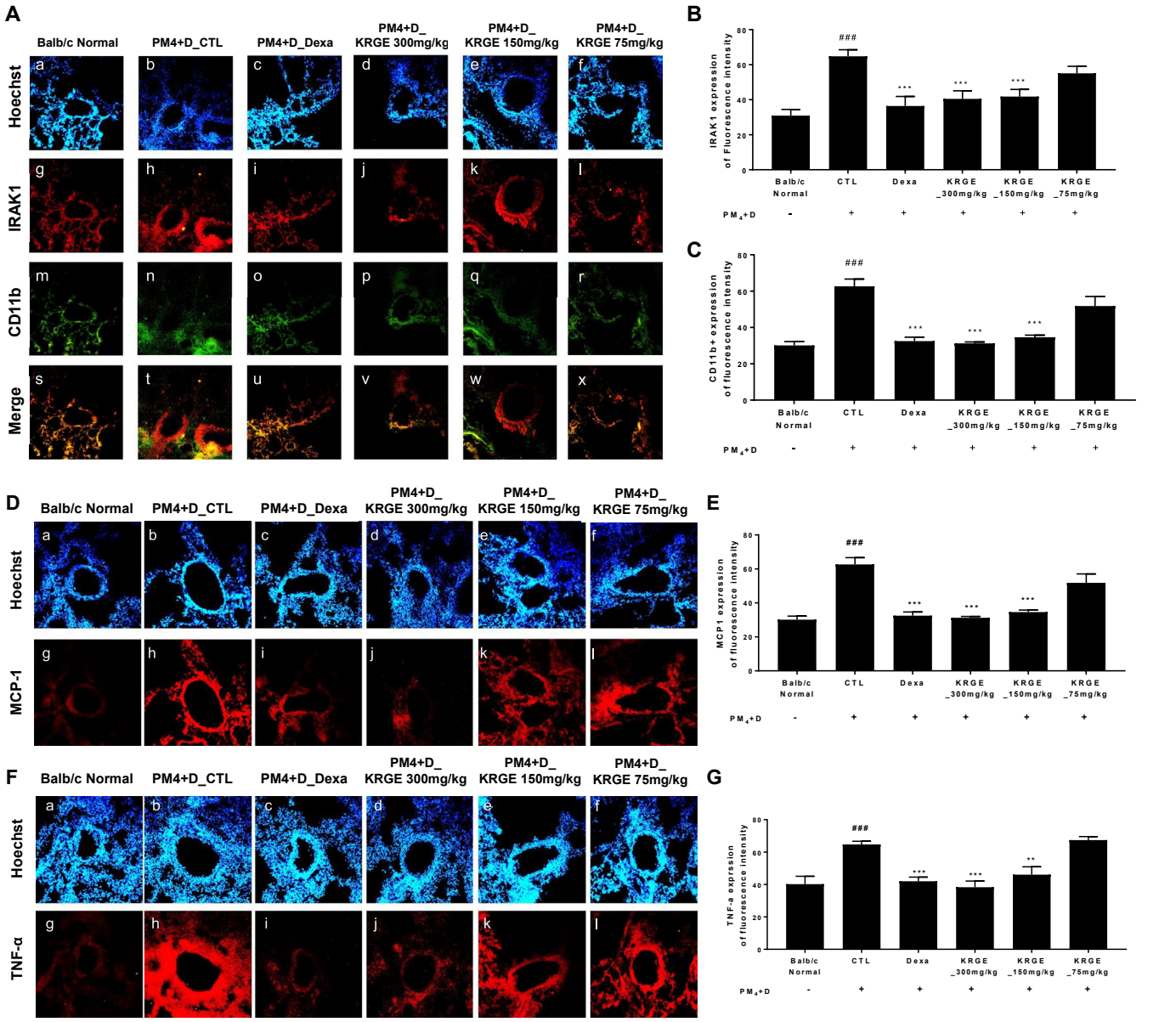

Fig. 5. Immunohistofluorescence (IHF) staining for IRAK1, CD11b, MCP-1, and TNF-α protein expression in lung tissues of a PM4+D-induced airway inflammation murine model. (A) IHF staining for IRAK1 (A-red), CD11b (A-green), merge (A-orange), Densitometric quantification of (B) IRAK1, (C) CD11b, (D) IHF staining for MCP-1 (D-red), and TNF-α (F-red) in lung tissues. Densitometric quantification of (E) MCP-1, and (G) TNF-α. Data are expressed as the mean ± SEM. BALB/c normal, PM4+D-sensitized control mice, 3 mg/kg dexamethasone-treated PM4+D-sensitized mice, 300 mg/kg KRGE-treated PM4+D-sensitized mice, 150 mg/kg KRGE-treated PM4+D-sensitized mice, and 75 mg/kg KRGE-treated PM4+D-sensitized mice.

antigen-specific cytotoxicity [32,33]. Gr-1/CD11b are expressed on the surfaces of granulocytes and some granulocytes, and are involved in the processes of inflammation, tumor growth, and cytotoxic T-cell inhibition [34,35]. These results indicate that the immune over activation caused by PM4+D was effectively suppressed by KRGE, thus inhibiting aggravation of inflammation. Cytokines, which are created by epithelial cells, endothelial cells, smooth muscle cells, fibroblasts, T lymphocytes, macrophages, and monocytes, are involved in the pathogenesis of PM-induced pulmonary diseases [36,37]. MIP2 plays an important role in mediating the neutrophilic inflammatory response to PM in rodent lungs, recruiting neutrophils and lymphocytes during inflammation, and is linked with the expression of adhesion molecules in bronchial epithelial cells and the production of chemotactic cytokines [38,39]. TNF-α, as a pleiotropic cytokine, is involved in growth promotion, growth inhibition, angiogenesis, cytotoxicity, inflammation, and immunomodulation, and has a key role in disease pathogenesis of pulmonary inflammation [40]. The chemokine CXCL1 and its receptor CXCR2 play crucial roles in the host immune response by activating neutrophils and subsequently promoting their adhesion to the endothelium [41]. Furthermore, PM interacts with immune cells in the airway and creates the infiltration of inflammatory cells and the production of oxidative stress that can directly activate TRPA1 and TRPV1 channels [42,43]. Pro IL-1a is bioactive when released from dying cells, and IL-1a is a major factor in particulate-induced acute lung inflammation [44]. The effects of this study diminished concentrations of MIP2, TNF-α, IL-17A, IL-1α and CXCL-1 in BALF, but also suppressed the gene expressions CXCL2, IL-17A, CXCL1, MUC5AC, IL-6, TNF-α, NOS-II, TRPA1 and TRPV1 in the lung of the PM4+D instillation model. These results

demonstrate that KRGE modulated the cytokine levels in the PM4+D-induced airway inflammation mouse model. In summary, KRGE inhibited the production of nitric oxide and the expression of pro-inflammatory mediators and cytokines through the MAPK/AP-1 pathways in PM4-stimulated MH-S cells. In addition, KRGE effectively alleviated lung tissue damage and inhibited airway inflammatory responses, such as granulocyte infiltration in the airway, by regulating the expression of chemokines and inflammatory cytokines in a PM4+D-induced airway inflammation mouse model. Therefore, we demonstrated respiratory disease prevention and protective effects of KRGE in PM4+D-induced airway inflammation. PM are recognized by Toll-like receptors and can act as ligands. TLRs are key pattern recognition receptors in innate immunity, which activate the NF-κB as well as IRAKs TAK-1. IRAKs and TKA-1 are key activator of NF-κB and MAPK/AP-1 pathways [43]. Elevated levels of NO, pro-inflammatory mediators and cytokines induced by PM4 were found to be suppressed by KRGE. In addition, KRGE inhibited the IRAKs and MAPK/AP-1 pathway in PM-4 induced MH-S cells, and decreased the IRAKs expression as well as NF-κB downstream factors CD11b, MCP-1 and TNF-α in lung of PM + D-induced airway inflammation model. These results suggest that KRGE may inhibit alveolar macrophage death and interleukin-1α release of pyroptosis pathway by PM + D-induced airway inflammation.

Acknowledgments

This work was funded by KOREA GINSENG CORP.

References

[1] Du W, Li X, Chen Y, Shen G. Household air pollution and personal exposure to air pollutants in rural China—a review. Environ Pollut 2018;237:625–38.
[2] Thompson JE. Airborne particulate matter: human exposure and health effects. J Occup Environ Med 2018;60(5):392–423.
[3] Gehring U, Wijga AH, Brauer M, Fischer P, Johan C de J, Kerkhof M, Henriette A Smit, Brunekreef B. Traffic-related air pollution and the development of asthma and allergies during the first 8 years of life. Am J Res 2010;181(6):596–603.
[4] Nkhama E, Ndhlovu M, Dvonch J, Lynam M, Mentz G, Siziya s, Voyi K. Effects of airborne particulate matter on respiratory health in a community near a cement factory in Chilanga, Zambia: results from a panel study. Int J Environ Res Publ Health 2017;14:1351.
[5] Mei M, Song H, Chen L, Hu B, Xu D, Liu Y, Zhao Y, Chen C. Early life exposure to three size-fractionated ultrafine and fine atmospheric particulates in Beijing exacerbates asthma development in mature mice. Part Fibre Toxicol 2018;13:15.
[6] Dufka M, Docekal B. Characterization of urban particulate matter by diffusive gradients in thin film technique. J Anal Method Chem 2018:9698710.
[7] Brunekreef B, Holgate ST. Air pollution and health. Lancet 2002;360:1233–42.
[8] Müller B, Seifart C, Barth PJ. Effect of air pollutants on the pulmonary surfactant system. Eur J Clin Invest 1998;28(9):762–77.
[9] Kim KH, Kabir E, Kabir S. A review on the human health impact of airborne particulate matter. Environ Int 2015;74:136–43.
[10] Dabass A, Talbott EO, Rager JR, Marsh GM, Venkat A, Holguin F, Shatma RK. Systemic inflammatory markers associated with cardiovascular disease and acute and chronic exposure to fine particulate matter air pollution (PM2.5) among US NHANES adults with metabolic syndrome. Environ Res 2018;61:485–91.
[11] Chen R, Li H, Cai J, Wang C, Lin Z, Liu C, Niu Y, Zhao Z, Li W, Kan H. Fine particulate air pollution and the expression of microRNAs and circulating cytokines relevant to inflammation, coagulation, and vasoconstriction. Environ Health Perspect 2018;126(1):017007.
[12] Kyung SY, Kim YS, Kim WJ, Park MS, Song JW, Yum H, Yoon HK, Rhee CK, Jeong SH. Guideline for the prevention and management of particulate matter/Asian dust particle-induced adverse health effect on the patients with pulmonary diseases. J Korean Med Assoc 2015;58(11):1060–9.
[13] Ernst E. Panax ginseng: an overview of the clinical evidence. J Ginseng Res 2010;34(2):259–63.
[14] Ro JY, Ahn YS, Kim KH. Inhibitory effect of ginsenoside on the mediator release in the Guinea pig lung mast cells activated by specific antigen-antibody reactions. Int J Immunol 1998;20(5):625–41.
[15] Wakabayashi C, Hasegawa H, Murata J, Saiki I. In vivo antimetastatic action of ginseng protopanaxadiolsaponins is based on their intestinal bacterial metabolites after oral administration. Oncol Res 1997;9(7):411–7.
[16] Choo MK, Sakurai H, Kim DH, Saiki I. A ginseng saponin metabolite suppresses tumor necrosis factor-alpha-promoted metastasis by suppressing nuclear factor-kappa B signaling in murine colon cancer cells. Oncol Rep 2008;19(1):595–600.
[17] Kim SN, Ha YW, Shin H, Son SH, Wu SJ, Kim YS. Simultaneous quantification of 14 ginsenosides in Panax ginseng Meyer by HPLC-ELSD and its application to quality control. J Pharm Biomed Anal 2007;45(1):164–70.
[18] Jung JH, Kang IG, Kim DY, Hwang YJ, Kim ST. The effect of Korean red ginseng on allergic inflammation in a murine model of allergic rhinitis. J Ginseng Res 2013;37(6):167–75.
[19] Yang Z, Chen A, Sun H, Ye Y, Fang W. Ginsenoside Rd elicits Th1 and Th2 immune responses to ovalbumin in mice. Vaccine 2007;25(1):161–9.
[20] Kim HS, Kim DH, Kim BK, Yoon SK, Kim MH, Lee JY, Kim HO, Park YM. Effects of topically applied Korean red ginseng and its genuine constituents on atopic dermatitis-like skin lesions in NC/Nga mice. Int Immunol 2011;11(4):280–5.
[21] Park EK, Choo MK, Kim EJ, Han MJ, Kim DH. Antiallergic activity of ginsenoside Rh2. Biol Pharm Bull 2003;26(3):1581–4.
[22] Zheng H, Jeong Y, Song J, Ji GE. Oral administration of ginsenoside Rh1 inhibits the development of atopic dermatitis-like skin lesions induced by oxazolone in hairless mice. Int Immunol 2011;11(4):511–8.
[23] Inoue K. Korean red ginseng for allergic rhinitis. Immunol Immunotoxicol 2013;35(1):693.
[24] Oh HA, Seo JY, Jeong HJ, Kim HM. Ginsenoside Rg1 inhibits the TSLP production in allergic rhinitis mice. Immunol Immunotoxicol 2013;35(4):678–86.
[25] Lee JR, Lee EO, Cha YY, Kang PA, IC RKYD, Ahn KS, Kim SH. Apoptotic effect of MC fraction of trichosanthis kirilowii maxim in human leukemic U937 cells. J Physiol Pathol Kor Med 2003;17(3):643–7.
[26] Curtis JL, Byrd PK, Warnock ML, Kaltreider HB. Requirement of CD4-positive T cells for cellular recruitment to the lungs of mice in response to a particulate intratracheal antigen. J Clin Invest 1991;88(4):1244–54.
[27] Walters DM, Breysse PN, Wills-Karp M. Ambient urban Baltimore particulate-induced airway hyperresponsiveness and inflammation in mice. Am J Respir Crit Care Med 2001;164:1438–43.
[28] Takano H, Yoshikawa T, Ichinose T, Miyabara Y, Imaoka K, Sagai M. Diesel exhaust particles enhance antigen-induced airway inflammation and local cytokine expression in mice. Am J Respir Crit Care Med 1997;156:36–42.
[29] Møller P, Danielsen PH, Karottki DG, Jantzen K, Roursgaard M, Klingberg H, Jensen DM, Christophersen DV, Hemmingsen JG, Cao Y, Loft S. Oxidative stress and inflammation generated DNA damage by exposure to air pollution particles. Mutat Res Rev Mutat 2014;762:133–66.
[30] Sarir H, Henricks PA, van Houwelingen AH, Nijkamp FP, Folkerts G. Cells, mediators and toll-like receptors in COPD. Eur J Pharmacol 2008;585:346–53.
[31] Harkema JR, Wagner JG, Kaminski NE, Morishita M, Keeler GJ, McDonald JD, Barrett EG, HEI Health Review Committee. Effects of concentrated ambient particles and diesel engine exhaust on allergic airway disease in Brown Norway rats. Res Rep Health Eff Inst 2009:5–55.
[32] Zamoyska R. CD4 and CD8: modulators of T-cell receptor recognition of antigen and of immune responses. Curr Opin Immunol 1998;10:82–7.
[33] Larosa DF, Orange JS. Lymphocytes. J Allergy Clin Immunol 2008;121:364–9.
[34] Choi JY, Oughton JA, Kerkvliet NI. Functional alteration in CD11b+Gr-1+ cells in mice injected with allogeneic tumor cells and treated with 2,3,7,8-tetrachlorodibenzo-p-dioxin. Int Immunopharm 2003;3:553–70.
[35] Lee JM, Seo JH, Kim YJ, Kim YS, Ko HJ, Kang CY. Agonistic anti-CD137 monoclonal antibody treatment induces $CD11b^{+}Gr\text{-}1^{+}$ myeloid-derived suppressor cells. Immune Netw 2010;10(3):104–8.
[36] Drisco ll KE. TNFalpha and MIP-2: role in particle-induced inflammation and regulation by oxidative stress. Toxicol Lett 2000;112–113:177–83.
[37] Gosset P, Lassalle P, Vanhée D, Wallaert B, Aerts C, Voisin C, Tonnel AB. Production of tumor necrosis factor-alpha and interleukin-6 by human alveolar macrophages exposed in vitro to coal mine dust. Am J Respir Cell Mol Biol 1991;5:431–6.
[38] Tavares E, Ojeda ML, Maldonado R, Miñano FJ. Neutralization of macrophage inflammatory protein-2 blocks the febrile response induced by lipopolysaccaride in rats. J Therm Biol 2004;29:413–21.
[39] Tsujimoto H, Ono S, Mochizuki H, Aosasa S, Majima T, Ueno C, Matsumoto A. Role of macrophage inflammatory protein 2 in acute lung injury in murine peritonitis. J Surg Res 2002;103:61–7.
[40] Matera MG, Calzetta L, Cazzola M. TNF-α Inhibitors in Asthma and COPD: we must not throw the baby out with the bath water. Pulm Pharmacol Therapeut 2010;23:121–8.
[41] Sawant KV, Xu R, Cox R, Hawkins H, Sbrana E, Kolli D, Garofalo RP, Rajarathnam K. Chemokine CXCL1-mediated neutrophil trafficking in the lung: role of CXCR2 activation. J Innate Immun 2015;7(6):647–58.
[42] Ogawa N, Kurokawa T, Mori Y. Sensing of redox status by TRP channels. Cell Calcium 2016;60(2):115–22.
[43] Falcon-Rodriguez CI, Osornio-Vargas AR, Sada-Ovalle I, Segura-Medin P. Aeroparticles, composition, and lung diseases. Front Immunol 2016;7:3.
[44] Yazdi AS, Guarda G, Riteau N, Drexler SK, Tardivel A, Couillin I, Tschopp J. Nanoparticles activate the NLR pyrin domain containing 3 inflammasome and cause pulmonary inflammation through release of IL-1a and IL-1b. Proc Natl Acad Sci USA 2010;107:19449–54. USA.